Journal of Hazardous Materials 428 (2022) 128251

Contents lists available at ScienceDirect

Journal of Hazardous Materials

journal homepage: www.elsevier.com/locate/jhazmat

Research Paper

Ozone for SARS-CoV-2 inactivation on surfaces and in liquid cell culture media

Chedly Tizaoui [a,*], Richard Stanton [b], Evelina Statkute [b], Anzelika Rubina [b], Edward Lester-Card [a], Anthony Lewis [a], Peter Holliman [a], Dave Worsley [a]

[a] College of Engineering, Bay Campus, Swansea University, Swansea SA1 8EN, United Kingdom
[b] Division of Infection & Immunity, School of Medicine, Cardiff University, Heath Park, Cardiff CF14 4XN, United Kingdom

HIGHLIGHTS

- Ozone reacted rapidly with SARS-CoV-2 at a rate constant of $\sim 7 \times 10^5$ M^{-1} s^{-1}.
- RH changed surface rate constant from 2.6×10^{-5} to 6.3×10^{-4} m^3/mg min
- RH = 70% was found plausible for dried SARS-CoV-2 inactivation by ozone
- Competitive reactions, mass transfer and virus occlusion could reduce inactivation

GRAPHICAL ABSTRACT

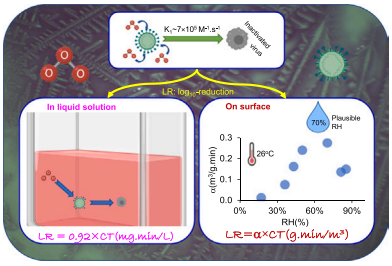

ARTICLE INFO

Editor: Dr. Danmeng Shuai

Keywords:
SARS-CoV-2
Ozone
Disinfection
Sanitisation
Virus

ABSTRACT

This study evaluated the inactivation of SARS-CoV-2, the virus responsible for COVID-19, by ozone using virus grown in cell culture media either dried on surfaces (plastic, glass, stainless steel, copper, and coupons of ambulance seat and floor) or suspended in liquid. Treatment in liquid reduced SARS-CoV-2 at a rate of 0.92 ± 0.11 log_{10}-reduction per ozone CT dose(mg min/L); where CT is ozone concentration times exposure time. On surface, the synergistic effect of CT and relative humidity (RH) was key to virus inactivation; the rate varied from 0.01 to 0.27 log_{10}-reduction per ozone CT value(g min/m^3) as RH varied from 17% to 70%. Depletion of ozone by competitive reactions with the medium constituents, mass transfer limiting the penetration of ozone to the bulk of the medium, and occlusion of the virus in dried matrix were postulated as potential mechanisms that reduce ozone efficacy. RH70% was found plausible since it provided the highest disinfection rate while being below the critical RH that promotes mould growth in buildings. In conclusion, through careful choice of (CT, RH), gaseous ozone is effective against SARS-CoV-2 and our results are of significance to a growing field where ozone is applied to control the spread of COVID-19.

1. Introduction

The Coronavirus Disease 2019 (COVID-19) is an infectious disease caused by the spread of the Severe Acute Respiratory Syndrome Coronavirus 2 (SARS-CoV-2) virus. With an average mortality rate of 2.2 death per 100 cases of COVID-19, the pandemic has caused over 3 million deaths (WHO, 2021) and resulted, throughout 2020, in a loss of 4.5% of the world gross domestic product (GDP) equivalent to almost

* Corresponding author.
E-mail address: c.tizaoui@swansea.ac.uk (C. Tizaoui).

https://doi.org/10.1016/j.jhazmat.2022.128251
Received 16 September 2021; Received in revised form 7 January 2022; Accepted 7 January 2022
Available online 10 January 2022

3.94 trillion US dollars (Szmigiera, 2021). Although vaccines are exceptionally efficient at preventing this serious disease, the selection of novel variants that are less well controlled by vaccination, and the slow rollout of vaccines in low-and-middle-income countries, mean that the virus remains a public health hazard worldwide.

SARS-CoV-2 spreads from person-to-person through inhalation of contaminated droplets and aerosols or by touching contaminated surfaces (i.e. fomites) (Mohan et al., 2021; Alimohammadi and Naderi, 2021). The virus remains viable in aerosols for up to 3 h, while on surfaces, it can remain viable up to 24 h (van Doremalen et al., 2020). By changing from winter to spring/fall environmental conditions, Kwon et al. showed that SARS-CoV-2 remains infectious on surfaces for up to 21 days and 7 days respectively, while it remained infectious for up to 3–4 days under indoor conditions (Kwon et al., 2021). In another study, Riddell et al. (2020) isolated viable virus from common surfaces after 28 days at 20 °C. Thus, these studies demonstrate the remarkable persistence of SARS-CoV-2 on surfaces under different environmental conditions highlighting the potential risk of contaminated surfaces as a driver of virus spread. Controlling the transmission of SARS-CoV-2 by eliminating the virus on surfaces and in liquid droplets and aerosols in the air is an important measure to curb COVID-19 disease.

In the recent year, a variety of methods have been studied to eliminate SARS-CoV-2 from the environment, including heat sterilisation, chemical disinfection, non-thermal plasma, and ultraviolet irradiation (Kwok et al., 2021; Martins et al., 2021; Volkoff et al., 2021; Welch et al., 2021; Oral et al., 2020; Murata et al., 2021). In these studies, the virus was inoculated onto a variety of hard and porous surfaces or in liquids before being exposed to the treatment. However, airborne virus studies are rare, due to the difficulty in safely handling aerosolised virus. Generally, the chemical disinfectants were either used in gas (e.g. ozone, hydrogen peroxide vapour) or liquid (e.g. chlorine-based agents, hydrogen peroxide) forms, with each offering advantages and disadvantages (Table 1). Being a gas and a strong oxidant, which can easily be produced from oxygen, ozone is more effective as compared to other chemical disinfectants. Ozone can also easily be applied in large and small areas and decompose back to safe oxygen after treatment. Ozone is particularly lethal against viruses through peroxidation of their surface lipids and subsequent damage to the lipid envelope and proteins

Table 1
Summary of effective disinfectants against SARS-CoV-2.

Technique	Advantages	Disadvantages	Potential areas of use	Typical doses for SARS-CoV-2 inactivation	References
Ozone	• A powerful disinfectant • Produced on site from oxygen in air • Can be easily converted back to oxygen using catalysts integrated in ozone generators • Gas, thus it can be distributed easily in space. • Low energy demand	• Inhalation at low concentration may increase health risk • Applied only in unoccupied environment • May generate by-products • High relative humidity is required when treating surfaces	Air, water, and surfaces	• Wide range of CT values from 100 s to 1000 s mg min/m^3 for surfaces • CT < 1 mg min/L for water.	(Martins et al., 2021; Volkoff et al., 2021; Murata et al., 2021; Tizaoui and Ozone, 2020; Zucker et al., 2021; De Forni et al., 2021)
UV	• Easy to operate • Chemical-free • Leaves no chemical residues • Damages the genomic system of microorganisms	• Unlikely to be feasible in large spaces indoor, hence with low impact • Light shielding • Sensitive to material type and ambient conditions (e.g. RH and T) • May generate ozone, if not controlled, • May present a risk to unprotected skin and eyes	Air, water, and surfaces	3–10 mJ/cm^2	(Raeiszadeh and Adeli, 2020; Minamikawa et al., 2021; Kitagawa et al., 2021)
Non thermal plasma	• Local disinfection	• High voltage • Reactive species may be toxic if not controlled (e.g. NOx, O_3) • Limited action in gas phase	Surfaces, liquids	< 20 min exposure time	(Bisag et al., 2020; Chen et al., 2020; Capelli et al., 2021)
Heat treatment	• Common method of disinfection in an autoclave	• Not suitable for materials sensitive to heat • Not suitable for indoor areas	Surfaces, liquids	30 min at 56 °C, < 10 min at > 70 °C	(Kwok et al., 2021; Xiling et al., 2021; Pastorino et al., 2020)
Sodium hypochlorite (chlorine bleach)	• Inexpensive • Widely available	• May attack materials, furniture, and electronic equipment • Hazardous to the environment • Sensitive to pH • Laborious to apply over large areas	Liquids, surfaces	150 ppm for 5 min	(Xiling et al., 2021; Brown et al., 2021; Subpiramaniyam, 2021)
Chlorine dioxide (liquid or gas)	• Can be produced onsite • Stronger disinfectant than sodium hypochlorite	• Inactivation takes place in wet state only • Requires high relative humidity in gas phase • Requires unoccupied spaces • Can be explosive	Liquids, surfaces, and air	~ 10 mg.min/L in water	(Kaly-Kullai et al., 2020; Morino et al., 2009)
Hydrogen peroxide (liquid or vapour)	• Safe at very low concentrations • Breaks down into molecular oxygen and water • Easily available (e.g. pharmaceutical grade solutions at 3% w/w)	• Modest virucidal activity • Acidification and additives are required • Long contact times and high concentrations are often necessary	Liquid or vapour	3% H_2O_2 + acetic acid for 5 min	(Mileto et al., 2021; Goyal et al., 2014; Schinkothe et al., 2021)

(Murray et al., 2008), and can also damage the capsid and genome (Kim et al., 1980; Wigginton and Kohn, 2012). Generally, the susceptibility of viruses to ozone depends on the type of virus, with enveloped viruses being more susceptible to ozone attack than non-enveloped viruses; this is due to the high reactivity of ozone with the lipid layer of the envelope (Tseng and Li, 2006; Tizaoui and Ozone, 2020). Being an enveloped virus, SARS-CoV-2 is therefore vulnerable to ozone attack through reactions with reactive oxygen species (ROSs) including molecular ozone and its decomposition products such as hydroxyl radicals and singlet oxygen (Tizaoui and Ozone, 2020; Li et al., 2016).

The efficacy of ozone gas to inactivate surface or airborne viruses depends on several operating factors including the product ozone concentration times exposure time (i.e. CT value - see Supplementary Information S1), the relative humidity (RH) (Hudson et al., 2009; Dubuis et al., 2020), the chemical composition of the media carrying the virus (i.e. water, biological fluid, aerosol, or dried/wet virus-adhered surface) (Araújo et al., 2013), and the type and texture of the surface (Szpiro et al., 2020). Although ozone has recently been studied to eliminate SARS-CoV-2 (Martins et al., 2021; Volkoff et al., 2021; Murata et al., 2021; Zucker et al., 2021; Yano et al., 2020; Uppal et al., 2021), these studies have only concerned with a narrow range of ozone dose and RH, and have mostly used surrogates instead of authentic SARS-CoV-2 virus (Zucker et al., 2021; Uppal et al., 2021). In addition, the effect of the media on virus inactivation has not been studied, and the CT values reported varied widely; for example, for a virus inactivation of 93% ± 3%, the reported CT values spanned over the range 0.1–40 g.min/m^3 (Murata et al., 2021; Zucker et al., 2021; Percivalle et al., 2021; Criscuolo et al., 2021). Furthermore, the effect of RH on inactivation has not been fully clarified, and there are no clear kinetic data on ozone-mediated inactivation of the virus.

To address these knowledge gaps and support possible large-scale field implementation of ozone for the elimination of SARS-CoV-2 from surfaces and in liquid medium, this paper aims to provide novel quantitative evidence on ozone inactivation of the causative virus of COVID-19. In particular, we used authentic SARS-CoV-2 virus to evaluate the synergistic effect of both CT and RH, and developed a unified basis to quantify their joint effect on virus inactivation by ozone. We evaluated the kinetics of virus inactivation and calculated rate constants in liquid and at different RH values. The effect of virus matrix was evaluated in liquid and dried media through reaction and mass transfer studies benchmarked against a probe of known reactivity with ozone, and the findings allowed us to suggest possible routes explaining the role of virus medium in interfering with the inactivation process.

2. Materials and methods

2.1. Cell lines and virus

VeroE6-ACE2 cells were generated by transducing VeroE6 cells (gifted by the University of Glasgow/MRC Centre for Virology, UK) with Lentivirus vectors expressing ACE2 followed by antibiotic selection. The England2 strain of SARS-CoV2 was provided by Public Health England. The virus was passaged at a low multiplicity of infection (MOI) of 0.01 in VeroE6 cells in Dulbecco's Modified Eagle Medium (DMEM). Virus containing supernatant was harvested at 72 h post-infection (hpi), before being stored at − 80 °C. The initial virus concentration was typically between 1×10^7 and 4×10^7 PFU/mL.

2.2. Quantification of virus

Virus infectivity was assessed by plaque assays. 10-fold serial dilutions were used to infect VeroE6 or VeroE6/ACE2/TMPRSS2 cells for 1 h, in duplicate. The cells were then overlaid with DMEM containing 2% FBS, and 1.2% Avicel® and incubated for 72 h. Following this, the overlay was removed, the cells were washed, fixed with 100% methanol and stained with 25% (v/v) methanol and 0.5% (v/v) Crystal Violet. The cell monolayer was then washed with water and plaques were counted.

2.3. Inactivation of SARS-CoV-2 by ozone

In the dried virus experiments, the tests involved drying a suspension of the virus (100 μL) onto a surface (mainly polystyrene plastic) under a gentle air stream in the biosafety cabinet for approximately 1 h. The obtained dried virus layer (approximately 1.5 cm × 1.5 cm) was then exposed to gaseous ozone inside a reactor (see 2.4 below). At the end of the experiment, the sample was reconstituted in 1 mL DMEM and infectious SARS-CoV-2 was quantified by plaque assay. The number of virus particles capable of forming plaques per unit volume (i.e. plaque-forming unit PFU/mL) were counted after ozone application and compared to a control exposed to air in the absence of ozone.

In the liquid experiments, 100 μL of DMEM virus solution was mixed with 100 μL of aqueous ozone solution or water (control) and was left to react before being titrated and plaques counted; typically, the initial ozone concentration was ~1 mg/L. In addition, liquid ozone solutions (1 mL, ~ 1 mg/L) were directly applied to dried virus samples; resuspension of a dried virus sample in 1 mL water was used as control. The suspensions were then titrated, and plaques counted.

The virus $\log_{10}$-reduction was calculated from the count of the surviving virus after exposure to ozone and the count of the control after exposure to air (or pure water) according to Eq. (1).

$$log_{10-}reduction = log_{10}\left(\frac{N_0}{N}\right) \quad (1)$$

Where: N is the count of the surviving virus per unit volume after ozonation and N_0 is the control virus count per unit volume.

2.4. The experimental reactor for viral exposure to ozone

The reactor used for exposing the virus to ozone was made of a 3 L plastic box fitted with a fan, a gas sampling port, a manual humidifier, a temperature and humidity probe, and an ozone supply canister (see Supplementary Information S2). The ozone canister was prepared by adsorbing ozone on silica gel and stored in a freezer at − 18 °C (see below Section 2.5). In an inactivation experiment, the ozone canister was collected from the freezer and immediately placed inside the reactor with the canister lid off and reactor cover on. As the opened canister is exposed to ambient conditions inside the reactor, ozone desorbs and occupies the headspace of the reactor while the fan ensures homogeneous distribution of the gas. The ozone concentration in the reactor was measured as outlined below (2.5).

2.5. Supply of ozone and gas concentration analysis

In this study, we developed new practical methods for ozone supply and analysis to avoid the use of specialised and complicated ozone equipment (i.e. ozone generator, a source of oxygen, an ozone analyser, valves, flow meters, pipes etc.), which is not practical in a category 3 biosafety laboratory (BSL-3). The supply of ozone was made from canisters containing ozone loaded on silica gel (typical mass of silica gel ~ 3 g) (Tizaoui and Slater, 2003). Briefly, the preparation of the canisters was made as follows: a 0.5 kg of silica gel (Sigma Aldrich, UK) of particle size of about 2–3 mm were packed in a glass column with gas inlet and outlet ports. Ozone was produced from pure oxygen (1 L/min) using an electrical ozone generator (BMT 803 N, BMT Messtechnik, Germany) and its gas concentration was measured with an ozone gas analyser (BMT964, BMT Messtechnik, Germany). The ozone adsorption was made at 0 °C and ozone gas concentration was typically 40 or 80 g/m^3 NTP (NTP: normal temperature and pressure). The ozone-loaded silica gel was then, carefully and rapidly, transferred into 8 mL glass vials (the canister) and immediately stored in a freezer at − 18 °C. The vials were transported in a car freezer (− 18 °C) from

Swansea University to Cardiff University, where they were stored in a lab freezer (− 18 °C) in readiness for the virus inactivation tests. Preliminary tests showed that ozone was stable while adsorbed on silica gel and stored under freezing conditions for over a month.

The ozone concentration in the gas phase (i.e. reactor headspace) was measured using a modified indigo trisulphonate method. Briefly, a 2 mL potassium indigo trisulphonate solution (Nobbs and Tizaoui, 2014) were withdrawn in a 10 mL syringe followed by the withdrawal of 8 mL of the ozone-containing gas from the reactor. The gas/liquid mixture was then thoroughly shaken and the change in absorbance at 600 nm of the indigo solution before and after exposure to ozone was measured using a UV/Vis spectrophotometer (Cary 60, Agilent). The ozone concentration was calculated using an indigo emissivity constant of 20,000 M^{-1} cm^{-1}. The ozone exposure CT value was calculated by integration of the measured ozone concentration as function of time.

2.6. Interference of virus culture media

To establish the extent of ozone quenching by the virus culture media in liquid and dry forms, DMEM samples (without virus) were exposed to ozone in the same manner as the inactivation experiments, but with slight modifications to account for larger sample analysis requirements. UV/Vis spectra were measured before and after ozonation using a UV/Vis spectrophotometer. A solution of indigo trisulphonate dye, used as a reference compound, was also exposed to ozone under the same conditions. Indigo dye was chosen as a reference because its reactivity with ozone is known ($k_{O3\text{-}indigo} = 9.4 \times 10^7$ M^{-1} s^{-1}; 1:1 stoichiometry) (Muñoz and von Sonntag, 2000), and also because it showed comparable reactivity to DMEM (see Section 3.2). In liquid form, a 1 mL DMEM solution (or indigo trisulphonate) was mixed with 1 mL ozone solution (~1 mg/L) and left to react for 5 min. In preliminary experiments, reaction times of 5 min were largely sufficient for this study due to the extremely rapid kinetics between ozone and DMEM (or indigo). In dry form, 600 μL of DMEM solution (or indigo trisulphonate solution) was dried on a glass petri dish overnight in the dark before being exposed to ozone in the gas reactor (or air as a control) for 20 min (4 canisters high ozone levels were used). After ozonation, the samples were reconstituted with 600 μL of DI water before their UV/Vis spectra were measured. In addition, ozone diffusion from the gas phase to the surface of a dried DMEM (or indigo) was evaluated and compared to a surface containing a liquid solution. For this, 8 mL of the DMEM solution were placed in a glass petri dish (diameter 6 cm) and exposed to ozone (or air as a control) for 20 min (1 ozone canister was used). Ozone concentration in the reactor's headspace and CT values were determined as described in 2.5 above. Photographs of dried samples were also taken to determine the surface area exposed to ozone, which permitted calculation of ozone flux and dose received by the dried sample.

2.7. Statistical analysis

The number of SARS-CoV-2 (PFU/mL) were counted and, after statistical analysis, the data were transformed to base10 logarithmic values. The mean and the standard error of the mean (i.e. standard deviation divided by the square root of the number of observations) were calculated and are reported graphically. The statistical significance of the results was evaluated at a confidence level $\geq 95\%$ (i.e. significance level $p \leq 0.05$). The One-Way ANOVA analysis of variance was used to compare the statistical differences in PFUs/mL numbers between control and ozone exposed samples. Differences were considered statistically significant when the *p*-value was ≤ 0.05. The function *anova1* of the Statistics and Machine Learning Toolbox in Matlab (Mathworks®, release R2020b) was used to perform the statistical analysis.

3. Results and discussion

3.1. Ozone analysis and supply

The method used in this study to determine ozone gas concentration in the reactor headspace by indigo trisulphonate (see 2.5) was validated against a calibrated ozone analyser (B12 Transmitter Ozone 0–5/200 ppm, ATI, UK); the difference between the indigo method and the calibrated analyser was less than 10% (see Supplementary Information S3). Ozone concentrations, by consequent CT values, were easily controlled from low to very high by simply changing the size (or number) of canisters (Fig. 1) or changing the ozone concentration used to prepare the canisters (data not shown). Typical changes of headspace ozone concentration as function of time are depicted in Fig. 1 at different ozone loadings in the absence (a) and in the presence (b) of virus sample. Fig. 1 shows that ozone transferred rapidly to the reactor headspace to reach a maximum concentration, C_0, followed by a slow decline in concentration in the absence of virus sample (Fig. 1(a)) but a rapid decline was observed when the reactor contained the virus sample (Fig. 1(b)). The rapid increase in ozone concentration in the reactor headspace was due to rapid release of ozone (i.e. desorption) from silica gel to the surrounding gas, while the depletion, observed in the absence of virus sample, was due to ozone self-decay in the gas phase. In the presence of virus sample, besides ozone depletion by self-decay reaction, ozone also diffuses from the headspace to the surface of the virus sample where it reacts, thereby its depletion rate was high as observed in Fig. 1 (b). A model accounting for these processes was developed and is presented in Supplementary Information (S4). Ozone depletion in the gas phase was assumed to proceed according an overall first-order reaction with an overall depletion rate constant, *K*, which was determined by fitting the experimental data with the model. Fig. 1 shows good agreement between the model (continuous red lines) and the experimental data (symbols) ($R^2 > 0.995$). The values of the ozone depletion rate constant in the absence and in the presence of virus samples were 0.020 ± 0.003 and 0.17 ± 0.016 min^{-1}, respectively, indicating that the ozone consumption was about 8 times higher in the presence of the virus solution. The high depletion rate in the presence of the virus sample was due to ozone consumption by the virus itself but also by constituents in the culture media that carry the virus; interference of the virus media is currently overlooked by published studies but can be significant (see next Section 3.2).

3.2. Interference of virus media on inactivation

The antiviral action of chemical disinfectants can be influenced by dissolved and surface-adhered organic and inorganic substances (Araújo et al., 2013; Gram et al., 2007), though, little is known about the interference of virus media on the antiviral action of ozone. Therefore, this study evaluated the extent of such effect on ozone reactivity, and mass transfer in both liquid and dried forms using indigo trisulphonate dye as a chemical reference compound.

In liquid solutions, the UV/Vis spectrum of DMEM changed significantly following mixing with the ozone solution at a similar removal percentage (25%) to that of indigo trisulphonate (29%) (Fig. 2 and Table 2). Both reactions were extremely rapid with no further reduction in absorbance at either 560 nm (for DMEM) or at 600 nm (for indigo trisulphonate) following analysis of the first sample ($t < 1$ min) indicating rapid uptake of ozone by the constituents of the DMEM. This suggests that in liquid form, the virus culture medium DMEM exerts a strong ozone demand and has a reactivity similar to that of indigo trisulphonate ($k = 9.4 \times 10^7$ M^{-1} s^{-1}) (Muñoz and von Sonntag, 2000). However, in the dry experiments, the removals of both DMEM and indigo trisulphonate were extremely low at percentages of 2% and 8% respectively (Table 2) indicating that sample drying resulted in significant inhibition of ozone reactions. To compare the uptake of ozone by a dried surface to a liquid surface, the results indicate that the removals

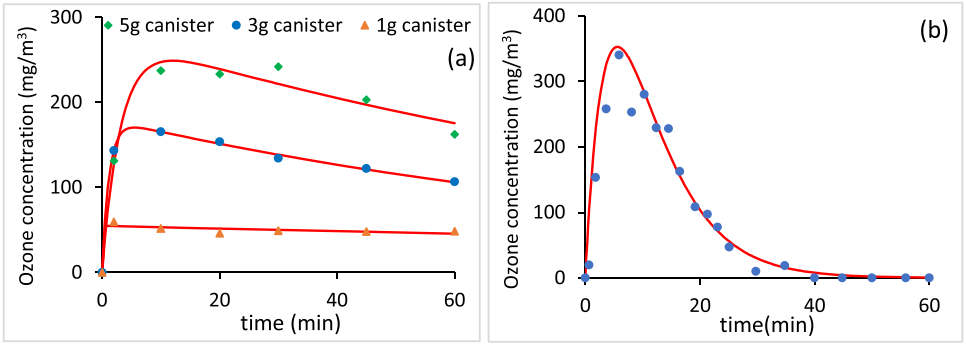

Fig. 1. Reactor headspace ozone concentrations: (a) at different masses of silica gel loaded with ozone (no virus); (b) in the presence of a dried virus sample. (For interpretation of the references to colour in this figure legend, the reader is referred to the web version of this article.)

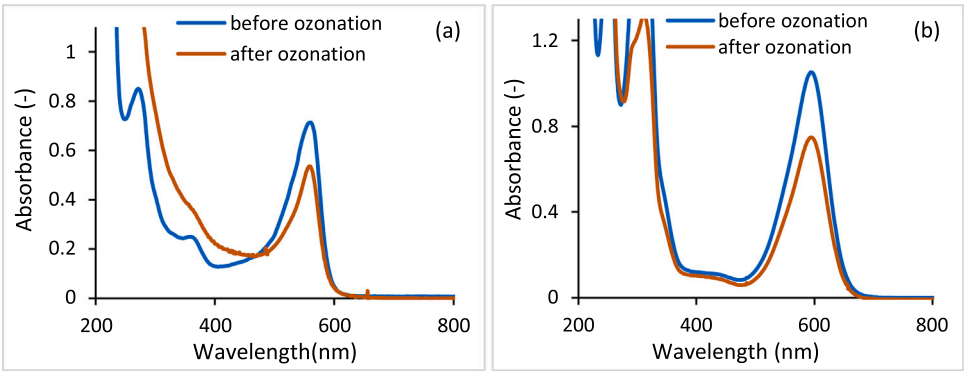

Fig. 2. Ozone oxidation of (a) DMEM and (b) indigo trisulphonate dye in liquid solutions (no virus).

Table 2
Ozone reactivity with liquid and dried media in the absence of virus (for gas above dried sample or above liquid solutions: ozone exposure time = 20 min, RH~50%).

Sample	Ozone in liquid sample (C = 1 mg/L)		Ozone gas above dried sample (CT = 14.5 g min/m^3)		Ozone gas above liquid sample (CT = 0.7 g min/m^3)	
	DMEM	Indigo	DMEM	Indigo	DMEM	Indigo
Removal[a]	25%	29%	2%	8%	50%	53%
Ozone flux per CT [(O_3molecules /cm^2 min)/ (g min/m^3)]	N/A		4.2×10^{12}		4.5×10^{14}	

[a] The removals of DMEM and indigo trisulphonate were calculated by the change in absorbance (Abs0-Abs)/Abs0 at 560 nm and 600 nm, respectively; where Abs0 is the initial absorbance and Abs is the absorbance after ozonation. For liquid mixtures of DMEM or indigo trisulphonate, Abs0 was determined by mixing the stock solution of either DMEM or indigo trisulphonate with DI water (without ozone) at the same volume ratio as the ozone experiment.

were much higher for a liquid surface at 50% DMEM and 53% indigo trisulphonate. These results further indicate that DMEM and indigo trisulphonate have similar reactivity with ozone. Comparing the diffusion rate of ozone transfer to a dried surface and a liquid surface, it was found that the rate of ozone diffusion to a dried surface was significantly lower by approximately 100 times to that of a liquid surface (Table 2). This suggests that viral inactivation of dried virus will require significantly high ozone doses that allow sufficient ozone transfer to reach the virus particles.

DMEM is a complex mixture containing inorganic salts (e.g. NaCl, $CaCl_2$, ferric, bicarbonate, phosphate etc.), amino acids (e.g. arginine, phenylalanine, tryptophan, tyrosine, glutamine etc.), vitamins (e.g. folic acid, thiamine, etc.), and glucose etc. The indigo trisulphonate solution also contained inorganics (phosphoric acid and sodium dihydrogen phosphate) in addition to the organic indigo trisulphonate dye. Thus, upon drying, the inorganic salts in solution crystallise (see Supplementary Information S5) and occlude the organic substances, providing protection from gaseous ozone attack. This is in line with disinfection studies, which showed that crystalline-type materials such as inorganic salts provide great protection to inactivation due to occlusion of microorganisms in crystals (Alfa et al., 1998, 1996; Höller et al., 1993). According to the obtained ratio of ozone mass transfer fluxes to dried and liquid surfaces, it could be suggested that for the same virucidal effect, gaseous ozone doses would be in the order of 100 times higher for inactivating dried virus than inactivating virus in liquid solutions. This suggestion was corroborated by a ratio of 60 for CT values, which is within the same order of magnitude as the ratio reported for ozone fluxes, obtained for dried and liquid media inactivation of φ6 bacteriophage by ozone (Tseng and Li, 2006, 2008). Ozone reacts rapidly with most of the constituents in DMEM solution, particularly the aromatic and sulphur-containing amino acids ($k_{O3} > 10^4$ M^{-1} s^{-1}) (Pryor et al., 1984), and as suggested earlier, the rate constant can be as high as that of indigo ~ 9.4×10^7 M^{-1} s^{-1}. Accordingly, the virus matrix would also impair virus inactivation through competition reactions.

Moreover, in liquid phase disinfection with gas, ozone must first transfer from the gas phase to the liquid phase before attacking the virus particles. Using liquid DMEM in conjunction with the reference indigo trisulphonate dye solution, our investigation showed that due to the high reactivity of ozone (demonstrated earlier), mass transfer controls the overall process and the reaction occurs entirely in the mass transfer liquid film with limited or no gas reaching the bulk fluid (Charpentier and Transfer, 1981).

In summary, our results suggest that interference of organic and inorganic substances on virus inactivation could occur through three different processes including mass transfer limitation, competitive

reactions, and occlusion of the virus in dried media. The first two processes are particularly relevant to virus inactivation in liquid solutions while the latter process is relevant to dried samples. Despite interference of the virus medium, ozone disinfection still occurs, albeit with reduced efficiency as demonstrated next.

3.3. Ozone inactivation of SARS-CoV-2

3.3.1. Virus inactivation in liquid DMEM

Aqueous ozone solutions were used to inactivate SARS-CoV-2 either suspended in liquid solutions (DMEM) or dried on a polystyrene plastic surface. At a low liquid ozone CT value (~ 0.1 mg.min/L), the application of aqueous ozone to suspended virus in DMEM led to only a small inactivation in virus titres (27%, $p = 0.022$) (Fig. 3). Others have achieved higher virus inactivation (99%) at similar CT value (Murata et al., 2021). However, they used a larger volume of ozone solution, which would also dilute out interfering substances. To increase virus inactivation, we increased the ozone dose by adding ozone-loaded silica gel (~ 0.04 g) directly to 2 mL virus solution for five minutes. Although the experiment continued for 5 min, the ozone concentration in solution depleted very fast (within 30 s); the CT value was estimated at 2.2 ± 0.2 mg.min/L. At this applied CT value, the virus inactivation increased significantly to 99%, $p = 0.018$ (Fig. 3). Having demonstrated effects on virus in solution, we next examined effects of ozonated water on surface-dried virus solution (i.e. a DMEM solution that contained the virus was dried in the biosafety cabinet by a gentle air stream followed by either resuspending the dried virus sample in aqueous ozone solution or in DI water or DMEM control experiments). The application of ozonated water on the surface containing initially dried virus solution at approximately CT = 0.5 mg.min/L yielded virus inactivation of 71%, $p = 0.010$ (Fig. 3) indicating that liquid ozone was also capable of inactivating dried virus on a surface. This latter experiment was in fact equivalent to exposing the virus in an aqueous ozone solution. This is because upon exposing the dried matrix to the liquid solution and with a quick swivel, the dissolution and resuspension of the substances was very fast, resulting in a well-mixed liquid solution where all constituents (i.e. virus and medium constituents) are exposed to ozone (also see Supplementary Information S6). Considering the results of virus inactivation in liquid form, the inactivation rate constant value (commonly used in water disinfection and is defined as the ratio $\log_{10}(N_0/N)$ over CT) was approximately 0.92 ± 0.11 $\log_{10}$-reduction per CT value (Fig. 3). In drinking water disinfection, this ratio is typically 10 $\log_{10}$-reduction per CT value (Rakness, 2005), which is approximately 10 times higher than the ratio obtained in our study. This could be explained by stronger ozone demand exhibited by the virus medium (i.e. DMEM) as compared to drinking water. Thus, high virus inactivation in solutions will require high ozone doses, to overcome the demand imposed by interfering substances.

We then used a modified Chick-Watson model (Lambert and Johnston, 2000), which assumes that the virus is inactivated by ozone at a rate governed by a rate constant K_1 and at the same time, ozone is quenched at a rate governed by a rate constant k_Q (see Supplementary Information S7). The rate constants K_1 and k_Q were determined by fitting of experimental data. Their values were $(7.2 \pm 0.98) \times 10^5$ M^{-1} s^{-1} and 30.3 ± 4.1 s^{-1} respectively (see Supplementary Information S7). The value of the virus inactivation rate constant, K_1, is in good agreement with rate constants reported for the inactivation of other viruses with ozone, which varied in the range 10^5 to 10^6 M^{-1} s^{-1} (Wolf et al., 2018). On the other hand, the magnitude of the ozone quenching rate constant indicates that the quenching reaction is very rapid and any increased inactivation times will lead to a maximum value of $\log_{10}$-reduction, which is dependent on the initial concentration of ozone, C_0, given by $K_1C_0/(2.3k_Q)$. Accordingly, to achieve, for example, 3 and 4 $\log_{10}$-reductions in the liquid solutions, the initial ozone concentrations need to be 15 and 20 mg/L, respectively. This simple model is of particular importance with respect to the disinfection of SARS-CoV-2 by ozone in liquid solutions since, for known kinetic parameters K_1 and k_Q (k_Q is media dependent), it allows predictions of virus inactivation and the effect that quenching substances impart to the disinfection process.

3.3.2. Gaseous ozone

3.3.2.1. Ozone inactivation of dried virus. To examine the ability of gaseous ozone to inactivate dried virus, 100 μL of the virus solution was dried onto the bottom of a polystyrene plastic well, then exposed to either ozone gas or air (control), for 3 min (CT = 0.5 g.min/m^3). Virus was then recovered and titrated, revealing that ozone gas inactivated the virus by only 23%, $p = 0.033$ (~ 0.12 $\log_{10}$ reduction) (Fig. 4). To enhance inactivation, the exposure time was increased to 5 and 20 min, consequently CT values increased to 1.0 and 4.7 g min/m^3, respectively. The measured virus inactivation values were 30%, $p = 0.022$% and 55%, $p = 0.015$ (Fig. 4), indicating the positive effect of CT. The dried matrix and relative humidity (RH ~ 40% in this experiment) affect the activity of ozone, which explains this modest inactivation. These inactivation percentages are comparable to recent results for the inactivation of SARS-CoV-2 surrogates (Zucker et al., 2021). To improve virus inactivation, we increased RH to ~ 70% and the CT values to ~ 5.0 g min/m^3 and ~ 15.0 g.min/m^3 (this was done by activating the manual humidifier inside the reactor and by increasing the number of ozone canisters), while keeping the experimental time short (< 1 h). It was crucial to keep the experimental time short, so virus inactivation due to "natural" decay of SARS-CoV-2 (Morris et al., 2020) did not interfere with the ozone inactivation. As CT increased to ~ 5.0 g min/m^3 and ~15.0 g.min/m^3, virus inactivation also

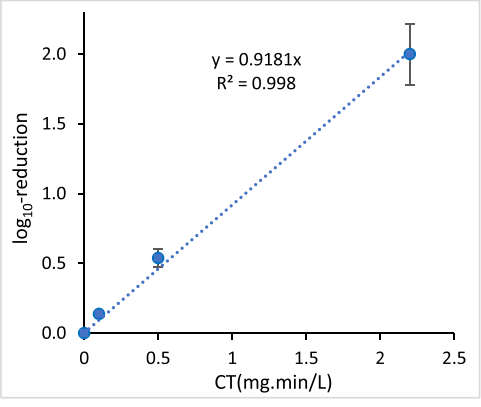

Fig. 3. SARS-CoV-2 inactivation by ozone in liquid solutions. Virus in DMEM; T = 26 °C. Standard error is shown by vertical bars.

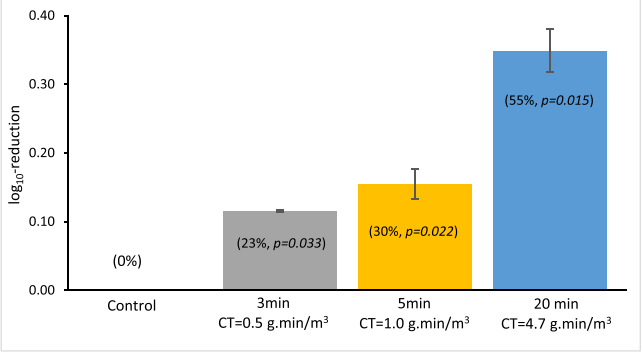

Fig. 4. Inactivation of dried SARS-CoV-2 at different exposure times (RH~40%, T = 26 °C; support surface: polystyrene plastic material; virus medium: DMEM). Virus inactivation percentages and p-values are shown between brackets. Standard error is shown by vertical bars.

significantly increased to 95%, $p = 0.0097\%$ and 99%, $p = 0.01$, respectively (Fig. 5). These results highlight the importance of CT values in inactivation and correspond well to those reported by other recent studies on coronaviruses and surrogates to SARS-CoV-2 who used similar virus matrix to ours (Murata et al., 2021; Zucker et al., 2021; Clavo et al., 2020). However, significantly lower CT values were reported by Yano et al. (2020). At average RH 70%, they reported that ozone CT values of only 0.1 and 0.7 g min/m^3 inactivated SARS-CoV-2 by 97% (1.5 $\log_{10}$-reduction) and 99.95% (3.3 $\log_{10}$-reduction) respectively. However, it's notable that they purified virus by ultrafiltration and three washing steps. Differences could therefore be attributed to virus medium composition variability, which, as demonstrated in this study, interfere significantly with ozone reactions in liquid and dried phases.

3.3.2.2. Effect of humidity. To evaluate the effect of humidity on the inactivation of surface-adhered virus, we treated dried samples of SARS-CoV-2 with ozone at different RH (17% to ~70%), while the ozone CT value was approximately 5.8 g min/m^3. The experimental results showed that as the relative humidity increased, the virus inactivation also increased (Fig. 6a-b), which is in agreement with literature (Tseng and Li, 2008). Mechanistic principles describing the influence of relative humidity on virus inactivation by gaseous ozone are not well developed. However, we drew upon the known effect of relative humidity on the decay of SARS-CoV-2, which follows an exponential decay model (van Doremalen et al., 2020; Marr et al., 2019), to suggest a minimal empirical correlation describing the effect of RH at a constant CT~5.8 g. min/m^3 (Eq. 2). The inactivation-RH plot (Fig. 6a) can be extrapolated to a zero inactivation to give a critical RH value of 13% below which ozone cannot inactivate the virus; a result which is consistent with literature (Dubuis et al., 2020). Although our experimental results highlight that an increase of RH yielded increased inactivation rates, other studies suggested that extremely high RH could reduce or increase the efficacy of ozone disinfection (Volkoff et al., 2021; Aydogan and Gurol, 2006). Thus, Eq. (2) is limited to RH < ~70% only.

The increased efficacy observed for RHs higher than the critical RH value could be explained by rehydration of the desiccated layer surrounding the virus, thereby enhancing ozone diffusion and virus exposure to the disinfectant; this is in line with the fact that ozone mass transfer rate was 100 times higher to a liquid surface as opposed to dried surface (see Section 3.2). Humidity, also promotes the decomposition of ozone to highly reactive species such as $^{\bullet}OH$, H_2O_2, $O_2^{\bullet-}$, and singlet oxygen, potentially increasing virus inactivation (Dubuis et al., 2020; Hudson et al., 2007). It can thus be concluded that humidity has a strong effect on disinfection of dried virus samples and its combination with ozone yields increased virus inactivation (Hudson et al., 2009; Elford and van den Ende, 1942). However, since extremely high RH could lead to either enhanced or reduced efficacy of ozone (Volkoff et al., 2021),

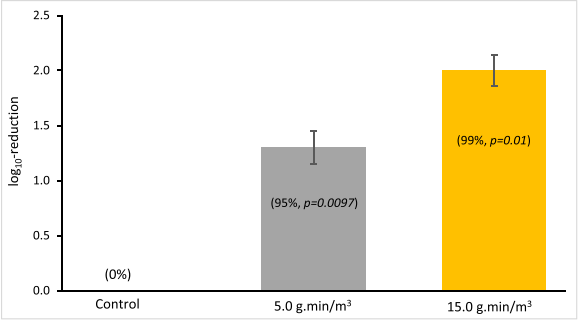

Fig. 5. Effect of gaseous ozone CT value on dried SARS-CoV-2 inactivation (RH~70%; T = 26 °C; support surface: polystyrene plastic material; virus medium: DMEM). Virus inactivation percentages and p-values are shown between brackets. Standard error is shown by vertical bars.

careful choice of RH should be made to ensure high inactivation rates. For example, Ishizaki, Shinriki and Matsuyama (Ishizaki et al., 1986) reported that an RH above 50% was required to inactivate Bacillus spores, while Bayarri et al. Bayarri et al. (2021) concluded that the best viral inactivation rates with ozone are achieved at RH between 70% and 90% only.

To establish the effect of RH on the virus inactivation kinetics, we determined the inactivation rate constant, *k*, at different relative humidities; *k* was calculated by $k = -\log_{10}(N/N_0)/CT$ (Supplementary Information S8). Starting from low values and increasing RH to approximately 70%, RH accelerated the inactivation rate by approximately 25 times. However, a further increase of RH above ~70% yielded a reduction in the inactivation rate constant (Supplementary Information S8). This might be due to accelerated ozone decomposition at high RH (Supplementary Information S9), which reduces the ozone concentration that reaches the surface where the disinfection process takes place. It could thus be concluded that humidification has the benefit of accelerating the ozone inactivation kinetics of dried SARS-CoV-2 but only up to a certain level, which was found RH= 70% in our experiments. This RH not only gives the highest inactivation rate constant, but it is also a plausible relative humidity since it is below the critical RH that promotes mould growth in buildings (>80% Viitanen et al. Viitanen et al., 2010).

$$Virus \quad Inactivation, \quad VI = 1 - \frac{N}{N_0} = 1 - 2.09exp[f_0](-5.68RH) \qquad (2)$$

Where Eq. (2) is valid for CT~5.8 g.min/m^3 and 13% < RH < 70%.

3.3.2.3. Synergistic effect of CT and RH. Our previous results show that ozone treatment of dried SARS-CoV-2 sample was mostly affected by the cooperative effect of CT and RH. To describe this synergy, we correlated the impact of CT and RH by isolines of inactivation percentages displayed in the contour plot on Fig. 7. Experimental results were complemented by model data points and Matlab (Mathworks®, release R2020b) was used for data processing and plotting. The results on Fig. 7 were determined for a temperature of 26 °C and virus dried in cell culture medium (DMEM). This condensed information can guide the selection of operational (CT, RH) to assist applications and research. Although DMEM was the medium used in this study, the conclusions of this investigation could be extrapolated to real fluids. For instance, both DMEM and saliva are made of 98–99% water and both media share a large number of organic and inorganic components (Engelen et al., 2007; Gibson and Beeley, 1994). Namely, both fluids contain sodium, potassium, calcium, bicarbonate, chloride and phosphate and share several organic molecules such as glucose, amino acids, cystine, glycine, and histidine compounds. Even though the concentrations of these substances vary, their occurrence in real biological fluids will, as demonstrated in DMEM, interfere with the virus inactivation process through competitive reactions, mass transfer limitation, and occlusion of the virus in crystallised materials (e.g. salts) upon drying. Thus, high RH (~ 70%) will remain an essential variable when treating dried real biological fluids with ozone while high CT doses will also remain an important requirement for high inactivation rates.

3.3.3. Inactivation of SARS-CoV-2 dried on different surface materials (gaseous ozone)

The effect of gaseous ozone on dried SARS-CoV-2 inactivation on different surface materials was also evaluated. Rigid nonporous (copper, stainless steel, and glass) and porous (coupons of ambulance seat and ambulance floor) surfaces were used. The surfaces were cleaned with water and acetone and dried before use. With copper, ambulance seat and ambulance floor, no viable virus could be recovered after treatment, even from the control sample. Copper is inherently antimicrobial and has been shown to inactivate SARS-CoV-2 within minutes (Bryant et al., 2021), while the porous ambulance seat and floor may have inactivated

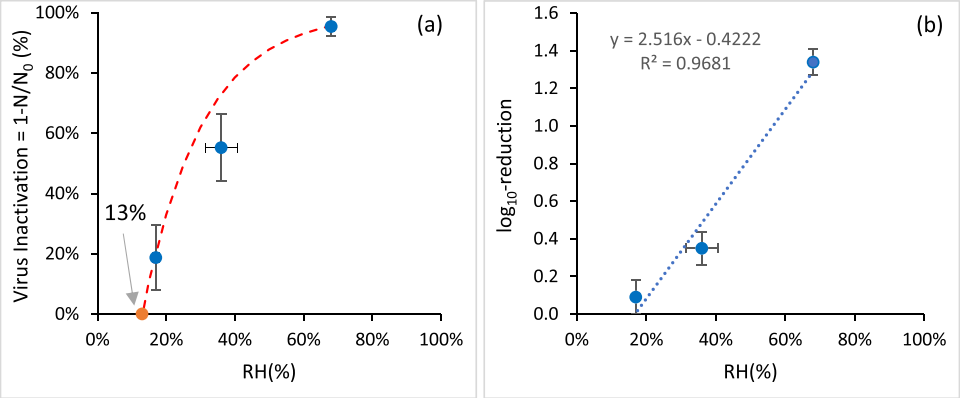

Fig. 6. Effect of relative humidity on dried SARS-CoV-2 inactivation with ozone in gas phase (T~26 °C, CT~5.8 g min/m^3, virus media: DMEM; support surface: polystyrene plastic material).

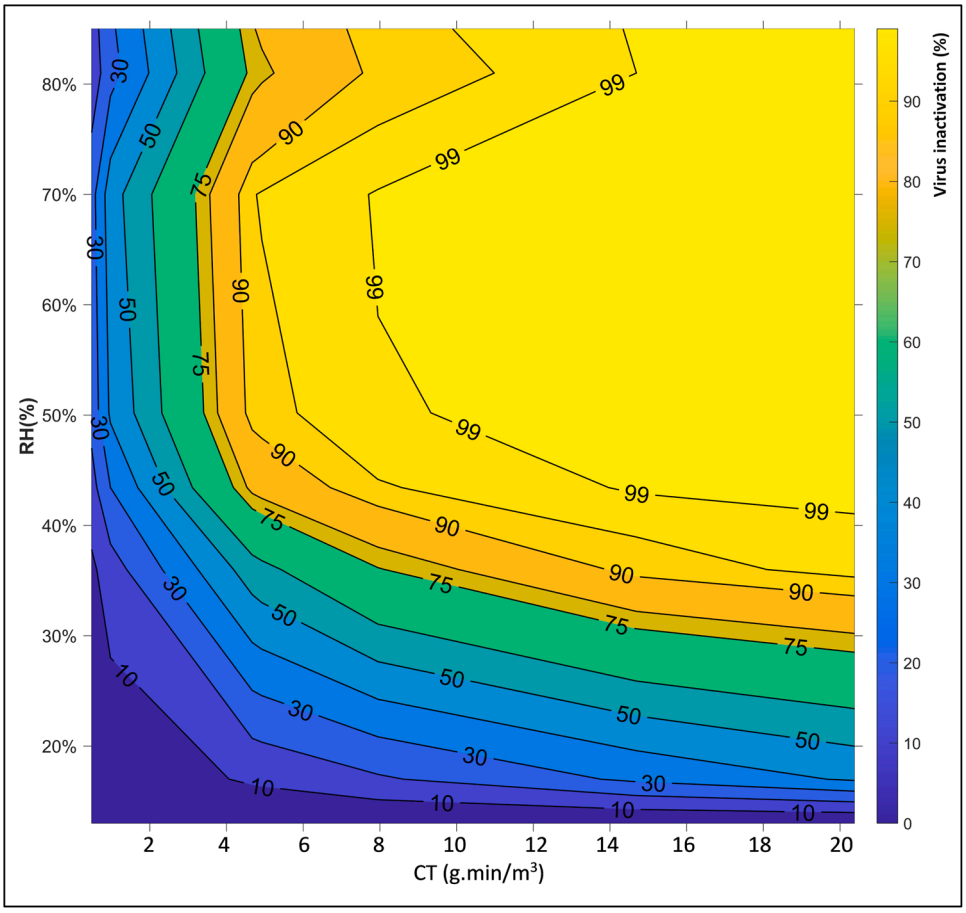

Fig. 7. Synergistic effect of (CT, RH) on dried SARS-CoV-2 inactivation by ozone gas. SARS-CoV-2 in cell culture media was dried on polystyrene plastic surface and exposed to ozone at different CT and RH% values (T = 26 °C).

the virus or trapped the remaining virus particles, preventing their elution during virus recovery. However, ozone effectively reduced infectious virus on both glass and steel by 99% (p-values < 0.05) (Fig. 8); this result is comparable to that on polystyrene plastic at the same CT and relative humidity (Fig. 7). Thus, virus inactivation on the rigid inert surfaces was not affected by the surface type, but inactivation on the porous materials or surfaces known to show antimicrobial effect should be examined.

4. Conclusions

This study demonstrated that ozone is effective for the inactivation of SARS-CoV-2 in liquid cell culture media and adhered on surfaces. In liquid solution, ozone was found to attack the virus rapidly at a rate constant of about 7×10^5 M^{-1} s^{-1}. The surface experiments demonstrated that both CT and RH have a synergistic effect on virus inactivation, with RH 70% was suggested as a plausible working relative humidity. Ozone mass transfer experiments demonstrated that the ozone flux to a liquid surface was 100 times higher than to a dried surface, which suggests that

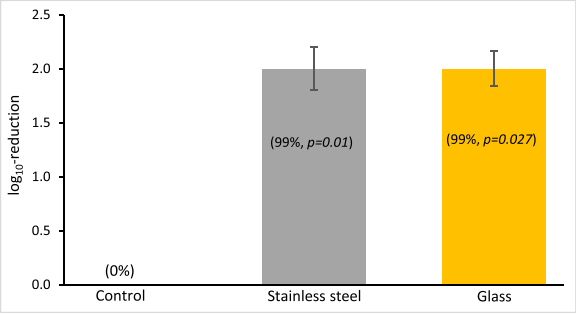

Fig. 8. SARS-CoV-2 inactivation by ozone on stainless steel and glass (100 μL of virus solution in DMEM was dried on SS or glass then exposed to ozone at RH 81%, T = 26 °C, CT~15.0 g min/m^3). Virus inactivation percentages and p-values are shown between brackets. Standard error is shown by vertical bars.

rehydration of dried virus medium at high RH enhanced virus exposure to ozone, thereby its inactivation. The results of virus medium effect suggested that the composition of the medium could limit viral inactivation through depletion of ozone by competitive reactions, mass transfer limiting the penetration of ozone to the bulk of the matrix, and potential occlusion of the virus in crystalline materials. In addition, this study demonstrated that the type of surface material affected virus inactivation. Specifically, rigid inert surfaces (stainless steel, glass, and plastic) gave similar virus inactivation by ozone whilst porous materials (ambulance seat and ambulance floor) or surfaces known to show antimicrobial effect (copper) inactivated the virus even in the absence of ozone. Moreover, this study correlated the synergistic effect of CT and RH in a contour plot to guide the selection of values for these important variables in ozone disinfection research and application studies.

As demonstrated in this study, the virus medium plays an important role in inhibiting virus inactivation, which suggests that future studies should further evaluate the elimination of the virus under different media conditions. The study also raised additional fundamental questions that are worthy investigating in the future. It is important to understand how constituents of the virus matrix affect virus shielding and how they affect ozone mass transfer to the bulk of the medium. Fundamental studies on the interaction between biological fluids and surface materials and how such interaction impacts virus inactivation by ozone in the presence of humidity are also worth pursuing in the future. In addition, studies on the inactivation of aerosolised SARS-CoV-2 by ozone, which are currently lacking, are worth pursuing given the importance of the airborne transmission route.

CRediT authorship contribution statement

Chedly Tizaoui: Conceptualization, Methodology, Formal analysis, Validation, Resources, Writing – original draft, Visualization, Supervision, Project administration, Funding acquisition. **Richard Stanton:** Conceptualization, Methodology, Validation, Resources, Writing – review & editing, Supervision, Project administration. **Evelina Statkute:** Validation, Formal analysis, Investigation, Data curation, Writing – review & editing. **Anzelika Rubina:** Validation, Formal analysis, Investigation, Data curation, Writing – review & editing. **Edward Lester-Card:** Formal analysis, Investigation, Writing – original draft. **Anthony Lewis:** Formal analysis, Investigation. **Peter Holliman:** Conceptualization, Methodology, Writing – review & editing, Supervision, Funding acquisition. **Dave Worsley:** Conceptualization, Methodology, Writing – review & editing, Supervision, Funding acquisition.

Declaration of Competing Interest

The authors declare that they have no known competing financial interests or personal relationships that could have appeared to influence the work reported in this paper.

Acknowledgements

This work was supported by the Welsh Government Small Business Research Initiative (SBRI) Centre of Excellence - Welsh Ambulance Service & Defence and Security Accelerator, United Kingdom (ACC2014616). The authors would like to thank Paula Toft, Ian Evans, Garry Tuckett and Paul Edwards at Swansea University for the help and support they provided throughout the course of this study over the lockdown period.

Appendix A. Supporting information

Supplementary data associated with this article can be found in the online version at doi:10.1016/j.jhazmat.2022.128251.

References

Alfa, M.J., DeGagne, P., Olson, N., Puchalski, T., 1996. Comparison of ion plasma, vaporized hydrogen peroxide, and 100% ethylene oxide sterilizers to the 12/88 ethylene oxide gas sterilizer. Infect. Control Hosp. Epidemiol. 17, 92–100.
Alfa, M.J., Olson, N., Degagne, P., Hizon, R., 1998. New low temperature sterilization technologies: microbicidal activity and clinical efficacy. In: Rutala, W.A. (Ed.), Disinfection, Sterilization, and Antisepsis in Healthcare. Polyscience Publications, New York, Champlain, New York, pp. 67–78.
Alimohammadi, M., Naderi, M., 2021. Effectiveness of ozone gas on airborne virus inactivation in enclosed spaces: a review study. Ozone-Sci. Eng. 43, 21–31.
Araújo, P.A., Lemos, M., Mergulhão, F., Melo, L., Simões, M., 2013. The influence of interfering substances on the antimicrobial activity of selected quaternary ammonium compounds. Int. J. Food Sci. 2013, 237581-237581.
Aydogan, A., Gurol, M.D., 2006. Application of gaseous ozone for inactivation of Bacillus subtilis spores. J. Air Waste Manag. Assoc. 56, 179–185.
Bayarri, B., Cruz-Alcalde, A., López-Vinent, N., Micó, M.M., Sans, C., 2021. Can ozone inactivate SARS-CoV-2? A review of mechanisms and performance on viruses. J. Hazard. Mater. 415, 125658.
Bisag, A., Isabelli, P., Laurita, R., Bucci, C., Capelli, F., Dirani, G., Gherardi, M., Laghi, G., Paglianti, A., Sambri, V., Colombo, V., 2020. Cold atmospheric plasma inactivation of aerosolized microdroplets containing bacteria and purified SARS-CoV-2 RNA to contrast airborne indoor transmission. Plasma Process. Polym. 17, 2000154.
Brown, J.C., Moshe, M., Blackwell, A., Barclay, W.S., 2021. Inactivation of SARS-CoV-2 in chlorinated swimming pool water. bioRxiv 2021, 440446, 2004.2019.
Bryant, C., Wilks, S.A., Keevil, C.W., 2021. Rapid inactivation of SARS-CoV-2 on copper touch surfaces determined using a cell culture infectivity assay. bioRxiv, 424974, 2021.2001.2002.
Capelli, F., Tappi, S., Gritti, T., Pinheiro, A., Laurita, R., Tylewicz, U., Spataro, F., Braschi, G., Lanciotti, R., Galindo, F.G., Siracusa, V., Romani, S., Gherardi, M., Colombo, V., Sambri, V., Rocculi, P., 2021. Decontamination of food packages from SARS-CoV-2 RNA with a cold plasma-assisted system. Appl. Sci. 11.
Charpentier, J.-C., Transfer, Mass, 1981. Rates in gas-liquid absorbers and reactors. In: Advances in Chemical Engineering. Academic Press, pp. 1–133.
Chen, Z., Garcia, G., Arumugaswami, V., Wirz, R.E., 2020. Cold atmospheric plasma for SARS-CoV-2 inactivation. Phys. Fluids 32, 6.
Clavo, B., Cordoba-Lanus, E., Rodriguez-Esparragon, F., Cazorla-Rivero, S.E., Garcia-Perez, O., Pinero, J.E., Villar, J., Blanco, A., Torres-Ascension, C., Martin-Barrasa, J. L., Gonzalez-Martin, J.M., Serrano-Aguilar, P., Lorenzo-Morales, J., 2020. Effects of ozone treatment on personal protective equipment contaminated with SARS-CoV-2. Antioxidants 9.
Criscuolo, E., Diotti, R.A., Ferrarese, R., Alippi, C., Viscardi, G., Signorelli, C., Mancini, N., Clementi, M., Clementi, N., 2021. Fast inactivation of SARS-CoV-2 by UV-C and ozone exposure on different materials. Emerg. Microbes Infect. 10, 206–210.
De Forni, D., Poddesu, B., Cugia, G., Gallizia, G., Licata, M.L., Lisziewicz, J., Chafouleas, J.G., Lori, F., 2021. Low ozone concentration and negative ions for rapid SARS-CoV-2 inactivation. bioRxiv 2021 (2003), 434968, 2011.
Dubuis, M.E., Dumont-Leblond, N., Laliberte, C., Veillette, M., Turgeon, N., Jean, J., Duchaine, C., 2020. Ozone efficacy for the control of airborne viruses: bacteriophage and norovirus models. PLoS One 15, 19.
Elford, W.J., van den Ende, J., 1942. An investigation of the merits of ozone as an aerial disinfectant. J. Hyg. 42, 240–265.
Engelen, L., van den Keybus, P.A.M., de Wijk, R.A., Veerman, E.C.I., Amerongen, A.V.N., Bosman, F., Prinz, J.F., van der Bilt, A., 2007. The effect of saliva composition on texture perception of semi-solids. Arch. Oral. Biol. 52, 518–525.
Gibson, J., Beeley, J.A., 1994. Natural and synthetic saliva: a stimulating subject. Biotechnol. Genet. Eng. Rev. 12, 39–62.
Goyal, S.M., Chander, Y., Yezli, S., Otter, J.A., 2014. Evaluating the virucidal efficacy of hydrogen peroxide vapour. J. Hosp. Infect. 86, 255–259.
Gram, L., Bagge-Ravn, D., Ng, Y.Y., Gymoese, P., Vogel, B.F., 2007. Influence of food soiling matrix on cleaning and disinfection efficiency on surface attached Listeria monocytogenes. Food Control 18, 1165–1171.
Höller, C., Martiny, H., Christiansen, B., Rüden, H., Gundermann, K.O., 1993. The efficacy of low temperature plasma (LTP) sterilization, a new sterilization technique. Zent. Hyg. Umw. 194, 380–391.

Hudson, J.B., Sharma, M., Petric, M., 2007. Inactivation of Norovirus by ozone gas in conditions relevant to healthcare. J. Hosp. Infect. 66, 40–45.
Hudson, J.B., Sharma, M., Vimalanathan, S., 2009. Development of a practical method for using ozone gas as a virus decontaminating agent. Ozone: Sci. Eng. 31, 216–223.
Ishizaki, K., Shinriki, N., Matsuyama, H., 1986. Inactivation of Bacillus spores by gaseous ozone. J. Appl. Bacteriol. 60, 67–72.
Kaly-Kullai, K., Wittmann, M., Noszticzius, Z., Rosivall, L., 2020. Can chlorine dioxide prevent the spreading of coronavirus or other viral infections? Medical hypotheses. Physiol. Int. 107, 1–11.
Kim, C.K., Gentile, D.M., Sproul, O.J., 1980. Mechanism of ozone inactivation of bacteriophage f2. Appl. Environ. Microbiol. 39, 210–218.
Kitagawa, H., Nomura, T., Nazmul, T., Kawano, R., Omori, K., Shigemoto, N., Sakaguchi, T., Ohge, H., 2021. Effect of intermittent irradiation and fluence-response of 222 nm ultraviolet light on SARS-CoV-2 contamination. Photo Photodyn. Ther. 33.
Kwok, C.S., Dashti, M., Tafuro, J., Nasiri, M., Muntean, E.A., Wong, N., Kemp, T., Hills, G., Mallen, C.D., 2021. Methods to disinfect and decontaminate SARS-CoV-2: a systematic review of in vitro studies. Ther. Adv. Infect. Dis. 8, 2049936121998548.
Kwon, T., Gaudreault, N.N., Richt, J.A., 2021. Environmental stability of SARS-CoV-2 on different types of surfaces under indoor and seasonal climate conditions. Pathogens 10, 7.
Lambert, R.J.W., Johnston, M.D., 2000. Disinfection kinetics: a new hypothesis and model for the tailing of log-survivor/time curves. J. Appl. Microbiol. 88, 907–913.
Li, Y., Zhang, C., Shuai, D.M., Naraginti, S., Wang, D.W., Zhang, W.L., 2016. Visible-light-driven photocatalytic inactivation of MS2 by metal-free g-C3N4: virucidal performance and mechanism. Water Res. 106, 249–258.
Marr, L.C., Tang, J.W., Van Mullekom, J., Lakdawala, S.S., 2019. Mechanistic insights into the effect of humidity on airborne influenza virus survival, transmission and incidence. J. R. Soc. Interface 16.
Martins, R.B., Castro, I.A., Pontelli, M., Souza, J.P., Lima, T.M., Melo, S.R., Siqueira, J.P. Z., Caetano, M.H., Arruda, E., de Almeida, M.T.G., 2021. SARS-CoV-2 inactivation by ozonated water: a preliminary alternative for environmental disinfection. Ozone: Sci. Eng. 43, 108–111.
Mileto, D., Mancon, A., Staurenghi, F., Rizzo, A., Econdi, S., Gismondo, M.R., Guidotti, M., 2021. Inactivation of SARS-CoV-2 in the liquid phase: are aqueous hydrogen peroxide and sodium percarbonate efficient decontamination agents? ACS Chem. Health Saf. 28, 260–267.
Minamikawa, T., Koma, T., Suzuki, A., Mizuno, T., Nagamatsu, K., Arimochi, H., Tsuchiya, K., Matsuoka, K., Yasui, T., Yasutomo, K., Nomaguchi, M., 2021. Quantitative evaluation of SARS-CoV-2 inactivation using a deep ultraviolet light-emitting diode. Sci. Rep. 11.
Mohan, S.V., Hemalatha, M., Kopperi, H., Ranjith, I., Kumar, A.K., 2021. SARS-CoV-2 in environmental perspective: occurrence, persistence, surveillance, inactivation and challenges. Chem. Eng. J. 405, 126893.
Morino, H., Fukuda, T., Miura, T., Lee, C., Shibata, T., Sanekata, T., 2009. Inactivation of Feline Calicivirus, a norovirus surrogate, by chlorine dioxide gas. Biocontrol Sci. 14, 147–153.
Morris, D.H., Yinda, K.C., Gamble, A., Rossine, F.W., Huang, Q., Bushmaker, T., Fischer, R.J., Matson, M.J., van Doremalen, N., Vikesland, P.J., Marr, L.C., Munster, V.J., Lloyd-Smith, J.O., 2020. The effect of temperature and humidity on the stability of SARS-CoV-2 and other enveloped viruses. bioRxiv, 341883, 2020.2010.2016.
Muñoz, F., von Sonntag, C., 2000. Determination of fast ozone reactions in aqueous solution by competition kinetics. J. Chem. Soc. Perkin Trans. 2, 661–664.
Murata, T., Komoto, S., Iwahori, S., Sasaki, J., Nishitsuji, H., Hasebe, T., Hoshinaga, K., Yuzawa, Y., 2021. Reduction of severe acute respiratory syndrome coronavirus-2 infectivity by admissible concentration of ozone gas and water. Microbiol. Immunol. 65, 10–16.
Murray, B.K., Ohmine, S., Tomer, D.P., Jensen, K.J., Johnson, F.B., Kirsi, J.J., Robison, R. A., O'Neill, K.L., 2008. Virion disruption by ozone-mediated reactive oxygen species. J. Virol. Methods 153, 74–77.
Nobbs, J., Tizaoui, C., 2014. A modified indigo method for the determination of ozone in nonaqueous solvents. Ozone: Sci. Eng. 36, 110–120.
Oral, E., Wannomae, K.K., Connolly, R., Gardecki, J., Leung, H.M., Muratoglu, O., Griffiths, A., Honko, A.N., Avena, L.E., McKay, L.G.A., Flynn, N., Storm, N., Downs, S.N., Jones, R., Emmal, B., 2020. Vapor H2O2 sterilization as a decontamination method for the reuse of N95 respirators in the COVID-19 emergency. medRxiv 2020, 20062026, 2004.2011.
Pastorino, B., Touret, F., Gilles, M., de Lamballerie, X., Charrel, R.N., 2020. Heat inactivation of different types of SARS-CoV-2 Samples: what protocols for biosafety, molecular detection and serological diagnostics? Viruses 12.
Percivalle, E., Clerici, M., Cassaniti, I., Vecchio Nepita, E., Marchese, P., Olivati, D., Catelli, C., Berri, A., Baldanti, F., Marone, P., Bruno, R., Triarico, A., Lago, P., 2021. SARS-CoV-2 viability on different surfaces after gaseous ozone treatment: a preliminary evaluation. J. Hosp. Infect. 110, 33–36.
Pryor, W.A., Giamalva, D.H., Church, D.F., 1984. Kinetics of ozonation. 2. Amino acids and model compounds in water and comparisons to rates in nonpolar solvents. J. Am. Chem. Soc. 106, 7094–7100.
Raeiszadeh, M., Adeli, B., 2020. A critical review on ultraviolet disinfection systems against COVID-19 outbreak: applicability, validation, and safety considerations. ACS Photonics 7, 2941–2951.
K.L. Rakness, Ozone in Drinking Water Treatment, American Water Works Association, Denver, USA, 2005.
Riddell, S., Goldie, S., Hill, A., Eagles, D., Drew, T.W., 2020. The effect of temperature on persistence of SARS-CoV-2 on common surfaces. Virol. J. 17, 145.
Schinkothe, J., Scheinemann, H.A., Diederich, S., Freese, H., Eschbaumer, M., Teifke, J. P., Reiche, S., 2021. Airborne disinfection by dry fogging efficiently inactivates severe acute respiratory syndrome Coronavirus 2 (SARS-CoV-2), mycobacteria, and bacterial spores and shows limitations of commercial spore carriers. Appl. Environ. Microbiol. 87.
Subpiramaniyam, S., 2021. Outdoor disinfectant sprays for the prevention of COVID-19: Are they safe for the environment? Sci. Total Environ. 759, 144289.
M. Szmigiera, 2021. Impact of the coronavirus pandemic on the global economy - Statistics & Facts. Avaialble at: ⟨https://www.statista.com/topics/6139/covid-19-impact-on-the-global-economy/⟩.
Szpiro, L., Pizzorno, A., Durimel, L., Julien, T., Traversier, A., Bouchami, D., Marie, Y., Rosa-Calatrava, M., Terrier, O., Moules, V., 2020. Role of interfering substances in the survival of coronaviruses on surfaces and their impact on the efficiency of hand and surface disinfection. medRxiv 2020, 2008.2022.20180042.
Tizaoui, C., 2020. Ozone: a potential oxidant for COVID-19 Virus (SARS-CoV-2). Ozone-Sci. Eng. 42, 378–385.
Tizaoui, C., Slater, M.J., 2003. Uses of ozone in a three-phase system for water treatment: ozone adsorption. Ozone: Sci. Eng. 25, 315–322.
Tseng, C., Li, C., 2008. Inactivation of surface viruses by gaseous Ozone. J. Environ. Health 70, 56–62.
Tseng, C.C., Li, C.S., 2006. Ozone for inactivation of aerosolized bacteriophages. Aerosol Sci. Technol. 40, 683–689.
Uppal, T., Khazaieli, A., Snijders, A.M., Verma, S.C., 2021. Inactivation of human coronavirus by FATHHOME's dry sanitizer device: rapid and eco-friendly ozone-based disinfection of SARS-CoV-2. Pathogens 10.
van Doremalen, N., Bushmaker, T., Morris, D.H., Holbrook, M.G., Gamble, A., Williamson, B.N., Tamin, A., Harcourt, J.L., Thornburg, N.J., Gerber, S.I., Lloyd-Smith, J.O., de Wit, E., Munster, V.J., 2020. Aerosol and surface stability of SARS-CoV-2 as compared with SARS-CoV-1. New Engl. J. Med.
Viitanen, H., Vinha, J., Salminen, K., Ojanen, T., Peuhkuri, R., Paajanen, L., Lahdesmaki, K., 2010. Moisture and bio-deterioration risk of building materials and structures. J. Build. Phys. 33, 201–224.
Volkoff, S.J., Carlson, T.J., Leik, K., Smith, J.J., Graves, D., Dennis, P., Aris, T., Cuthbertson, D., Holmes, A., Craig, K., Marvin, B., Nesbit, E., 2021. Demonstrated SARS-CoV-2 surface disinfection using ozone. Ozone-Sci. Eng.
Welch, J.L., Xiang, J., Mackin, S.R., Perlman, S., Thorne, P., O'Shaughnessy, P., Strzelecki, B., Aubin, P., Ortiz-Hernandez, M., Stapleton, J.T., 2021. Inactivation of severe acute respiratory coronavirus virus 2 (SARS-CoV-2) and diverse RNA and DNA viruses on three-dimensionally printed surgical mask materials. Infect. Control Hosp. Epidemiol. 42, 253–260.
WHO, 2021. COVID-19 Weekly Epidemiological Update (21 March 2021) available at ⟨https://www.who.int/publications/m/item/weekly-epidemiological-update-on-covid-19—23-march-2021⟩.
Wigginton, K.R., Kohn, T., 2012. Virus disinfection mechanisms: the role of virus composition, structure, and function. Curr. Opin. Virol. 2, 84–89.
Wolf, C., von Gunten, U., Kohn, T., 2018. Kinetics of Inactivation of Waterborne Enteric Viruses by Ozone. Environ. Sci. Technol. 52, 2170–2177.
Xiling, G., Yin, C., Ling, W., Xiaosong, W., Jingjing, F., Fang, L., Xiaoyan, Z., Yiyue, G., Ying, C., Lunbiao, C., Liubo, Z., Hong, S., Yan, X., 2021. In vitro inactivation of SARS-CoV-2 by commonly used disinfection products and methods. Sci. Rep. 11, 2418.
Yano, H., Nakano, R., Suzuki, Y., Nakano, A., Kasahara, K., Hosoi, H., 2020. Inactivation of severe acute respiratory syndrome coronavirus 2 (SARS-CoV-2) by gaseous ozone treatment. J. Hosp. Infect. 106, 837–838.
Zucker, I., Lester, Y., Alter, J., Werbner, M., Yecheskel, Y., Gal-Tanamy, M., Dessau, M., 2021. Pseudoviruses for the assessment of coronavirus disinfection by ozone. Environ. Chem. Lett.